Directional Locking and the Role of Irreversible Interactions in Deterministic Hydrodynamics Separations in Microfluidic Devices

Manuel Balvin, Eunkyung Sohn, Tara Iracki, German Drazer,* and Joelle Frechette†

Department of Chemical and Biomolecular Engineering, Johns Hopkins University, Baltimore, Maryland 21218, USA

(Received 24 April 2009; published 11 August 2009)

We performed macroscopic experiments on the motion of a sphere through an array of obstacles that highlight the deterministic nature of the lateral displacements that lead to particle separation in microfluidic systems. The motion of the spheres is irreversible and displays directional locking. The locking directions can be predicted with a single parameter that distinguishes between reversible and irreversible particle-obstacle collisions. These results stress the need to incorporate irreversible interactions to predict the movement of a non-Brownian sphere passing through a periodic array.

DOI: 10.1103/PhysRevLett.103.078301 PACS numbers: 47.57.E−, 05.45.−a, 05.60.Cd, 82.70.Dd

The potential technological impact of lab-on-a-chip technologies for analytical chemistry has propelled the need for separation methods that are rapid, effective, and continuous [1–4]. One strategy to achieve separation in microfluidic devices has been the miniaturization of well-established macroscale methods (such as size exclusion and hydrodynamic chromatography). While effective, these techniques are characterized (and limited) by the random nature of the pore space, which implies that the separative displacement of different species is the average behavior of an inherently stochastic process. Alternatively, microfabrication has opened the door to new concepts for separation, such as deterministic hydrodynamics, in which the components being fractionated become locked into size-dependent periodic trajectories that exhibit lateral migration as they travel through an array of obstacles [5]. This and similar techniques have been employed for the fractionation of whole blood components [6], the assessment of platelet size [7], and the fractionation of particles via optical traps [8–10].

The separation principles involved in deterministic hydrodynamics are not well-understood. The proposed mechanism is based on the streamlines followed by a simple fluid at low Reynolds numbers (Stokes flow) and in the absence of suspended particles [5,11]. Thus, it does not include hydrodynamic or nonhydrodynamic interactions between the particles and the obstacles, or possible inertia effects. A better understanding of the phenomena underlying the observed separation is needed to further develop this promising method. Investigations in the regime of high Peclet numbers would truly explore deterministic behavior and would showcase the underlying physical mechanism causing separation.

We conducted simple experiments using a large array of obstacles and a uniform driving force (gravity) to explore the deterministic nature of the *deterministic hydrodynamics* separation method. We investigate the motion of stainless steel balls falling through a periodic array of obstacles created with cylindrical LEGO® pegs on a LEGO® board and immersed in a transparent tank filled with glycerol. The pegs have a radius $R = 3.9$ mm and are located on a 12×17 square lattice with lattice spacing $l = 16$ mm. The board could be rotated to vary the forcing angle θ relative to the principal directions of the obstacle array. We used stainless steel balls of density 7.75 $\mathrm{g\,cm^{-3}}$ with radii $a =$ 1.5 mm, 3 mm, 3.18 mm, and 3.55 mm. Delrin particles of density 1.4 $\mathrm{g\,cm^{-3}}$ and $a = 3.18$ mm were also employed. The difference between the largest and the smallest diameter measured in a single ball was less than 3 μm for all the particles. The estimated Reynolds number for the largest particles is $\mathrm{Re} = 0.7$. (see Ref. [12])

The particles follow periodic trajectories that exhibit directional locking into lattice directions. In Fig. 1(a) we show the periodic motion resulting from the directional locking of the particles into the (1,2) lattice direction. Note that the forcing angle is $\theta = 30°$, which shows that the average motion, $\alpha = \arctan(1/2) = 26.57°$, is not collinear with the external force. While both 3 mm and 6 mm spheres move in the same direction on average, their periodic trajectories are not identical within a single lattice cell. The periodicity of the trajectories is demonstrated in Fig. 1(b), showing the collapse of multiple trajectories projected into a single period. The periodic trajectory followed by the particles is independent of the column of the array in which the balls entered the system. We also tracked several 6 mm particles in which we intentionally changed the entry point within a single unit cell and obtained the same asymptotic trajectory [Fig. 1(c)]. The collapse of the trajectories into a unique periodic motion, that is independent of initial position within a unit cell and acts as a limit-cycle, is a direct observation that the evolution of the system is not (time) reversible and, therefore, cannot be described with purely hydrodynamic interactions in the Stokes limit [13–16]. Evidence of irreversible motion has also been reported recently by Austin's group [11]. Finally, in Fig. 1(d) we show the trajectories obtained for a forcing angle $\theta = 13°$ for which we observe separation of the 3 mm balls from the 6 and 7.1 mm spheres.

The average migration angle plotted against the orientation of the external force is presented in Fig. 2 for spheres

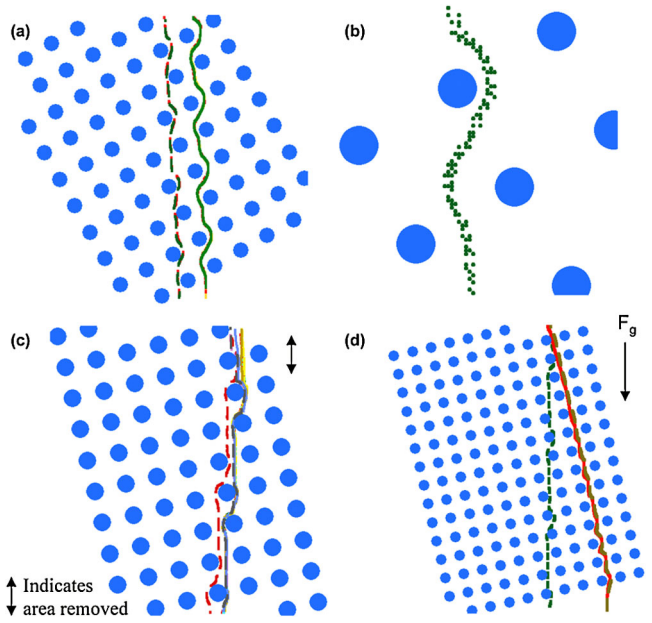

FIG. 1 (color online). Trajectories for: (a) 3 mm and 6 mm spheres with directional locking into the (1,2) direction at a forcing angle of 30°; (b) a single period, obtained by translating all the periods of different 6 mm sphere trajectories; (c) trajectories of 6 mm spheres entering at different points in the array. All trajectories locked into the (1,2) direction for a forcing angle of 13.5°. (d) Trajectories of 3 mm (green dotted line), 6 mm (red dashed line), and 7.1 mm (grey solid line) spheres. The 3 mm sphere locked into the (1,4) direction, whereas the 6 mm and 7.1 mm spheres locked into the (0,1) direction. The forcing angle was 13°.

of 3, 6 and 7.1 mm radii. In all cases we observe a Devil's staircase type of structure, consisting of plateaus and steps, that is characteristic of directional locking systems [17,18]. The plateaus correspond to particular lattice directions that are preferentially selected over specific ranges of force orientations. The observed transitions between locking directions are relatively smooth, in contrast to the expected sharp transitions typical of phase-locking systems. In these transition regions, however, we were able to identify portions of the trajectory in which the particle is locally moving at one of the two corresponding migration angles. For example, with the LEGO® board oriented at a forcing angle of 16.2° the 3 mm balls transition from being locked into the (1,4) lattice direction for smaller angles to locked motion in the (1,3) lattice direction. In this case there are segments in which the particle moved in the (1,3) direction and portions in which the average motion was in the (1,4) direction. We calculate the probability to move in each direction by counting the number and size of the associated segments and obtained that, in all cases, the two directions associated with the transition account for more than 90% probability (see Ref. [12]). Note, however, that dividing the trajectory in segments of any length is arbitrary, in that what we define as segments could actually be part of a periodic trajectory with a much larger period and a single migration angle.

Several forcing angles can be found for which different particles will move in different directions. Moreover, some of the spheres exhibited locked-in states that the other spheres did not, such as the (1,4) lattice direction for the 3 mm balls or the motion in the (2,3) lattice direction exhibited only by the 3 mm and the 6 mm balls but not the 7.1 mm balls. We also observe that the first critical angle, at which the ball becomes unlocked from the (0,1) lattice direction, shows a strong dependence on particle size. In fact, we used the first critical forcing angles to separate the particles shown in Fig. 1(d).

The complex dependence of the migration angle on the driving force shown in Fig. 2 can be reproduced with a simple two-particle model that we introduced previously [19]. In agreement with the present experiments our simulations showed that, in the presence of short-ranged, nonhydrodynamic interactions between the moving sphere and the solid obstacles, particles moved in (uniquely determined) periodic trajectories and exhibited directional locking. We then approximated the motion inside the obstacle array by a series of independent collisions between the moving sphere and the obstacles. Each of the hydrodynamic collisions is then classified as irreversible or reversible depending on whether they induce or not a net lateral displacement in the trajectory of the moving particle. The simulations showed that the magnitude of the induced lateral displacement can be described in terms of a single parameter, the critical impact parameter b_c shown in Fig. 3. If the incoming impact parameter b_{in} is larger than b_c the

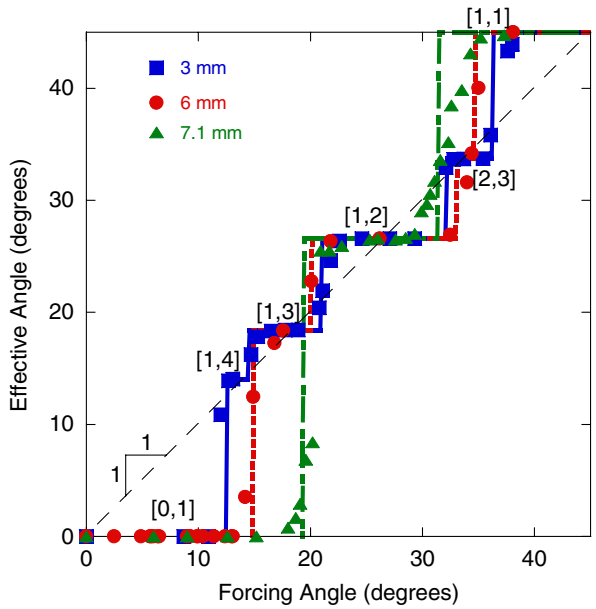

FIG. 2 (color online). Effective angles as a function of the orientation of the driving force. The simulation results best fit the experiments with 3 mm (solid blue), 6 mm (dotted red), and 7.1 mm (dashed green) spheres when $b_c = 2.30$ (3.5 mm), 1.36 (4.1 mm), and 1.48 (5.3 mm), respectively.

collision trajectory is symmetric, but all collisions with $b_{\text{in}} < b_c$ collapse into a single outgoing trajectory that corresponds to the symmetric collision with $b_{\text{out}} = b_c$. This irreversible collapse of a finite range of incoming trajectories into a single outgoing trajectory leads to periodic motion and phase-locking dynamics [20]. The critical impact parameter fully determines the migration angle for a given forcing direction and is a measure of the asymmetry induced by the irreversible interactions present in the system, such as forces resulting from solid contact due to roughness or electrostatic repulsion. (Note that our simulations considered spherical obstacles, in contrast to the cylindrical obstacles used in the experiments.) In Fig. 2 we also compare the experimental results with the two-particle collision model discussed above, with b_c as the only fitting parameter. The excellent agreement between the experimental data and the simulations indicates that this (simple) model is able to capture the complex dynamics of the system.

Finally, to confirm that (reversible) Stokes dynamics cannot reproduce the observed behavior, we performed a set of experiments in which we used particles of the same size (6.35 mm diameter) but of different densities (stainless steel vs plastic balls). While the driving force and the velocity of the particles will be affected by a change in particle density, in the Stokes limit both particles should follow the exact same path for all forcing angles. The external force is proportional to the density difference between the solid balls and the suspending fluid and thus, will be different for the two types of particles. In the Stokes limit, however, the velocity vector is a linear function of the driving force (through a second order tensor). Therefore, a change in the magnitude of the force will only change the speed of a falling particle but not its trajectory. On the other hand, if the trajectory of the particles depends on their density, other factors such as nonhydrodynamic effects or inertia must be playing a role. As shown in Fig. 4, the observed phase locking is clearly different for the two particles, thus demonstrating that Stokes hydrodynamics fails to predict the observed behavior. Experiments were performed for both types of particles simultaneously to avoid any difference in the forcing angles.

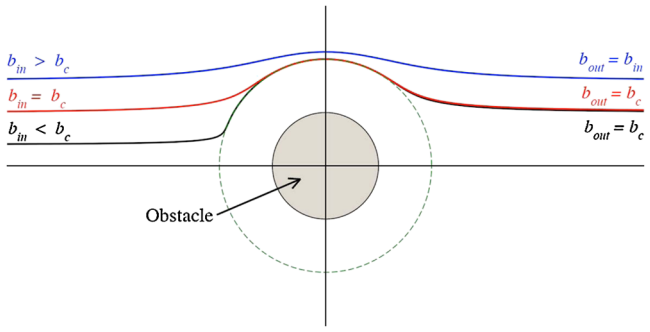

FIG. 3 (color online). Schematic view of the different trajectories resulting from the collision of a freely suspended sphere (particle), on which a constant external force is applied, with a sphere that remains fixed at the center (obstacle). The symmetry of the particles trajectory is broken if the incoming impact parameter (b_{in}) is less than the critical impact parameter (b_c) (see the text).

The results presented here confirm the presence of directional locking in deterministic systems at low Reynolds numbers. The migration angle as a function of the forcing direction exhibits a Devil's staircase type of structure, common to many phase-locking systems. The observed trajectories are periodic and as a consequence the migration angles always correspond to a lattice direction. Also, different particles might move in different lattice directions for specific values of the forcing angle, resulting in separation. The observed behavior is completely analogous to that observed in microfluidic systems that induce size-based separation by deterministic lateral displacement. The reported trajectories in these microfluidic devices are periodic and also indicate the presence of directional locking. Specifically, the authors observe the transition from a locked state in the (0,1) direction for large particles (displacement mode in Refs. [5,6,21]) to a locked angle that is substantially closer to the flow direction for smaller particles (zigzag mode in Refs. [5,6,21]). The fact that the orientation of the force in Ref. [5] coincides with the (1,10) lattice direction makes it impossible to determine whether the reported zigzag mode would actually follow the flow for any forcing direction, as suggested by the authors. Finally, the separation in these devices also seems to take advantage of the first critical angle, which according to the present results is the most sensitive to particle

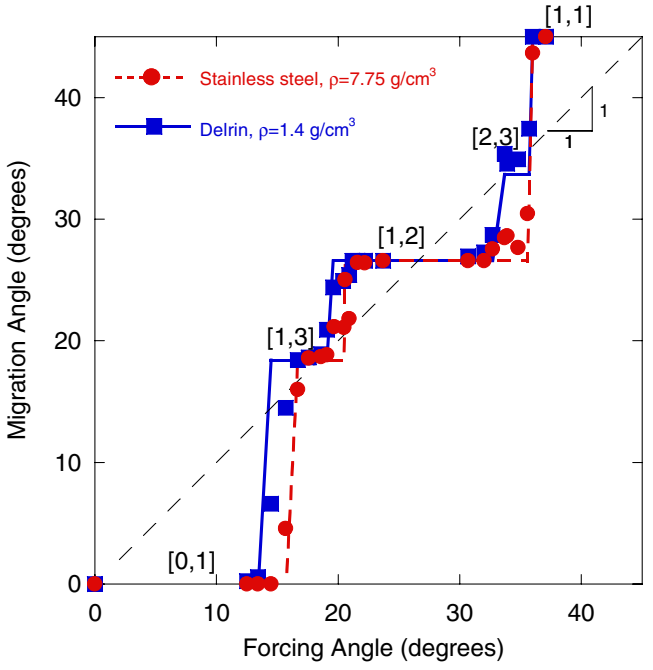

FIG. 4 (color online). Migration angle vs forcing angle for particles of the same size ($a = 3.18$ mm) but with different densities. The symbols correspond to the average migration angle. The lines correspond to the most probable angle.

size. However, there are important differences between our work and these microfluidic systems. First of all, and except for the work in Ref. [5], the patterns of obstacles are not the rotation of a square lattice, but a series of rows of obstacles that are shifted in the lateral direction. In addition, we use a uniform driving force (gravity) while microfluidic devices commonly employ other driving fields (electrophoretic fields or pressure-driven flows). However, these other driving fields would lead to analogous behavior in the presence of irreversible particle-obstacle interactions, i.e., the presence of symmetric or nonsymmetric trajectories depending on the impact parameter of the collision. Changing the driving force could change b_c for a given particle-obstacle pair, but given a value of b_c there is a unique phase-locking curve associated with it, independent of the driving field.

General design guidelines for the implementation of this separation principle towards microfluidic devices can be drawn from our work. First, the first critical angle exhibits a strong dependence on the particle size, making it the most promising angle for separation purposes (see Fig. 2). Second, it is likely that the lateral displacement is governed by short-range interactions that scale with interacting area (interplay between hydrodynamic lubrication and nonhydrodynamic surface forces). As a result, the first critical angle should increase with particle size, which is consistent with our experimental results. Therefore, the obstacle size has to be chosen to maximize the relative change in interaction areas between the different particle sizes and obstacles. Finally, it is likely that the value of the forcing angle will need to be chosen without an *a priori* knowledge of the value of the critical impact parameter for all the particle sizes in the system. In this likely scenario one can choose a forcing angle by assuming an equal probability distribution for the value of b_c for each particle size. Based on our observations and in the numerical results presented in Ref. [19], we can assume that the critical collision parameter is typically between $b_c = R/2$ and $b_c = a_i + R$, where R is the obstacle size and a_i is the size of the particle. Note that the first transition occurs when the critical impact parameter becomes equal to the lateral displacement between successive rows of obstacles, $b_c = l\sin(\theta)$. The chance of separation between two different particles is then maximized for a forcing angle $l\sin(\theta) = (3R + a_1 + a_2)/4$. The forcing angles obtained from this probability analysis should provide a good starting point for the design of an array for separation. For our experiments, we would obtain $\theta \approx 15°$ to separate 7.1 mm and 6 mm particles from 3 mm spheres, and $\theta \approx 17°$ to separate between 7.1 mm and 6 mm particles, which compares well with our experimental results (see Fig. 2).

We have shown that the presence of irreversible interactions between the moving particle and the obstacle disrupts the symmetry of the trajectory, inducing a net lateral displacement. Even though the resulting lateral displacement is typically small, the periodic nature of the system allows such lateral displacement to accumulate, thus amplifying the effect into a macroscopic change in the migration angle. Therefore, by controlling weak, short-range, nonhydrodynamic forces, such as electrostatic forces, microfluidic devices employing periodic arrays should be able to enhance the separation of species.

This material is partially based upon work supported by the National Science Foundation under Grant No. CBET-0731032. Acknowledgment is made to the Donors of the American Chemical Society Petroleum Research Fund for partial support of this research under Grants No. 46510G5 and No. 46514G9.

*drazer@jhu.edu
†jfrechette@jhu.edu

[1] M. P. MacDonald, G. C. Spalding, and K. Dholakia, Nature (London) **426**, 421 (2003).
[2] J. El-Ali, P. K. Sorger, and K. F. Jensen, Nature (London) **442**, 403 (2006).
[3] P. Yager, T. Edwards, E. Fu, K. Helton, K. Nelson, M. R. Tam, and B. H. Weigl, Nature (London) **442**, 412 (2006).
[4] D. Janasek, J. Franzke, and A. Manz, Nature (London) **442**, 374 (2006).
[5] L. R. Huang, E. C. Cox, R. H. Austin, and J. C. Sturm, Science **304**, 987 (2004).
[6] J. A. Davis, D. W. Inglis, K. J. Morton, D. A. Lawrence, L. R. Huang, S. Y. Chou, J. C. Sturm, and R. H. Austin, Proc. Natl. Acad. Sci. U.S.A. **103**, 14779 (2006).
[7] D. W. Inglis, K. J. Morton, J. A. Davis, T. J. Zieziulewicz, D. A. Lawrence, R. H. Austin, and J. C. Sturm, Lab Chip **8**, 925 (2008).
[8] P. T. Korda, M. B. Taylor, and D. G. Grier, Phys. Rev. Lett. **89**, 128301 (2002).
[9] A. M. Lacasta, J. M. Sancho, A. H. Romero, and K. Lindenberg, Phys. Rev. Lett. **94**, 160601 (2005).
[10] A. Gopinathan and D. G. Grier, Phys. Rev. Lett. **92**, 130602 (2004).
[11] K. Loutherback, J. Puchalla, R. H. Austin, and J. C. Sturm, Phys. Rev. Lett. **102**, 045301 (2009).
[12] See EPAPS Document No. E-PRLTAO-103-015934 for a discussion of experimental setup, materials, and methods. For more information on EPAPS, see http://www.aip.org/pubservs/epaps.html.
[13] R. H. Davis, Phys. Fluids **4**, 2607 (1992).
[14] M. L. Ekiel-Jezewska, F. Feuillebois, N. Lecoq, K. Masmoudi, R. Anthore, F. Bostel, and E. Wajnryb, Phys. Rev. E **59**, 3182 (1999).
[15] G. Drazer, J. Koplik, B. Khusid, and A. Acrivos, J. Fluid Mech. **460**, 307 (2002).
[16] G. Drazer, J. Koplik, B. Khusid, and A. Acrivos, J. Fluid Mech. **511**, 237 (2004).
[17] P. Bak, Phys. Today **39**, No. 12, 38 (1986).
[18] C. Reichhardt and F. Nori, Phys. Rev. Lett. **82**, 414 (1999).
[19] J. Frechette and G. Drazer, J. Fluid Mech. **627**, 379 (2009).
[20] J. Herrmann, M. Karweit, and G. Drazer, Phys. Rev. E **79**, 061404 (2009).
[21] D. W. Inglis, J. A. Davis, R. H. Austin, and J. C. Sturm, Lab Chip **6**, 655 (2006).